Functional Segregation of a Predicted "Hinge" Site within the β-Strand Linkers of *Escherichia coli* Leucyl-tRNA Synthetase†

Anjali P. Mascarenhas and Susan A. Martinis*

Department of Biochemistry, University of Illinois, 600 South Mathews Avenue, 419 Roger Adams Laboratory, Box B-4, Urbana, Illinois 61801-3732

Received December 20, 2007; Revised Manuscript Received February 22, 2008

ABSTRACT: Some aminoacyl-tRNA synthetases (AARSs) employ an editing mechanism to ensure the fidelity of protein synthesis. Leucyl-tRNA synthetase (LeuRS), isoleucyl-tRNA synthetase (IleRS), and valyl-tRNA synthetase (ValRS) share a common insertion, called the CP1 domain, which is responsible for clearing misformed products. This discrete domain is connected to the main body of the enzyme via two β-strand tethers. The CP1 hydrolytic editing active site is located ~30 Å from the aminoacylation active site in the canonical core of the enzyme, requiring translocation of mischarged amino acids for editing. An ensemble of crystal and cocrystal structures for LeuRS, IleRS, and ValRS suggests that the CP1 domain rotates via its flexible β-strand linkers relative to the main body along various steps in the enzyme's reaction pathway. Computational analysis suggested that the end of the N-terminal β-strand acted as a hinge. We hypothesized that a molecular hinge could specifically direct movement of the CP1 domain relative to the main body. We introduced a series of mutations into both β-strands in attempts to hinder movement and alter fidelity of LeuRS. Our results have identified specific residues within the β-strand tethers that selectively impact enzyme activity, supporting the idea that β-strand orientation is crucial for LeuRS canonical core and CP1 domain functions.

Aminoacyl-tRNA synthetases (AARSs)[1] are ancient enzymes that are responsible for covalently linking specific amino acids to their cognate tRNAs (*1*). The family of AARSs "charge" tRNA by covalently linking it to an amino acid via a two-step aminoacylation reaction. The enzyme binds adenosine triphosphate (ATP) and an amino acid (AA) to form an aminoacyl−adenylate intermediate with release of pyrophosphate (PP). The activated amino acid is then transferred to the 2′- or 3′-ribose hydroxyl of the tRNA's terminal adenosine to form an aminoacyl-tRNA. Charged tRNA is delivered to the ribosome where the attached amino acid is incorporated into protein.

The AARSs have evolved different strategies for achieving high fidelity and preventing the misincorporation of an incorrect amino acid during translation (*2, 3*). Certain amino acids, such as cysteine and tyrosine, have unique side chains that are readily recognized at the molecular level (*4*). However, isosteric sets of amino acids that differ by a single methyl group (i.e., isoleucine and valine or alanine and glycine) are not easily distinguished (*5*). Thus, at least half of the AARSs have evolved amino acid editing mechanisms to clear mistakes (*2, 3*). A noncognate amino acid mischarged to the wrong tRNA isoacceptor can be cleared via a post-transfer editing mechanism which cleaves the amino acid from the tRNA. Alternatively, pretransfer editing hydrolyzes misactivated adenylate intermediates (*6, 7*).

Class I LeuRS, IleRS, and ValRS have highly homologous aminoacylation and editing domains (*8*). Within their canonical Rossmann fold cores where the aminoacylation active site resides, these enzymes have an ~190-residue insert that folds into a large independent domain (*9–11*), termed CP1 (connective polypeptide 1) (*12*). The CP1 domain is tethered to the main body of the enzyme via two flexible β-strand linkers (Figure 1). This insert houses the enzyme's editing active site, which is responsible for clearing mischarged amino acids.

More than 25 crystal structures of the homologous LeuRS, IleRS, and ValRS display different orientations that the CP1 domain adopts to accommodate aminoacylation and post-transfer editing complexes as well as intermediate states. These multiple orientations of the CP1 domain during various stages of the enzyme's cycle would require flexibility of the β-strands linking the CP1 domain to the canonical core. Comparison of apo *Thermus thermophilus* LeuRS (*13*) to the cocrystal structure of the aminoacylation complex of *Pyrococcus horikoshii* LeuRS with $tRNA^{Leu}$ shows that the CP1 domain swings ~20° relative to the canonical core of the enzyme to prevent a clash with the bound 5′ terminus of tRNA (*14*). Subsequent to aminoacylation, the 3′ end of the tRNA is translocated ~30 Å from the synthetic active site to the amino acid editing site for proofreading, requiring the editing domain to rotate by ~35° compared to the apo state of *T. thermophilus* LeuRS (*13*). The exit complex

† This work was supported by National Institutes of Health Grant GM063789.

* To whom correspondence should be addressed. Phone: (217) 244-2405. Fax: (217) 244-5858. E-mail: martinis@life.uiuc.edu.

[1] Abbreviations: AARS, aminoacyl-tRNA synthetase; LeuRS, leucyl-tRNA synthetase; CP1, connective polypeptide 1.

10.1021/bi702494q CCC: $40.75
Published on Web 03/26/2008

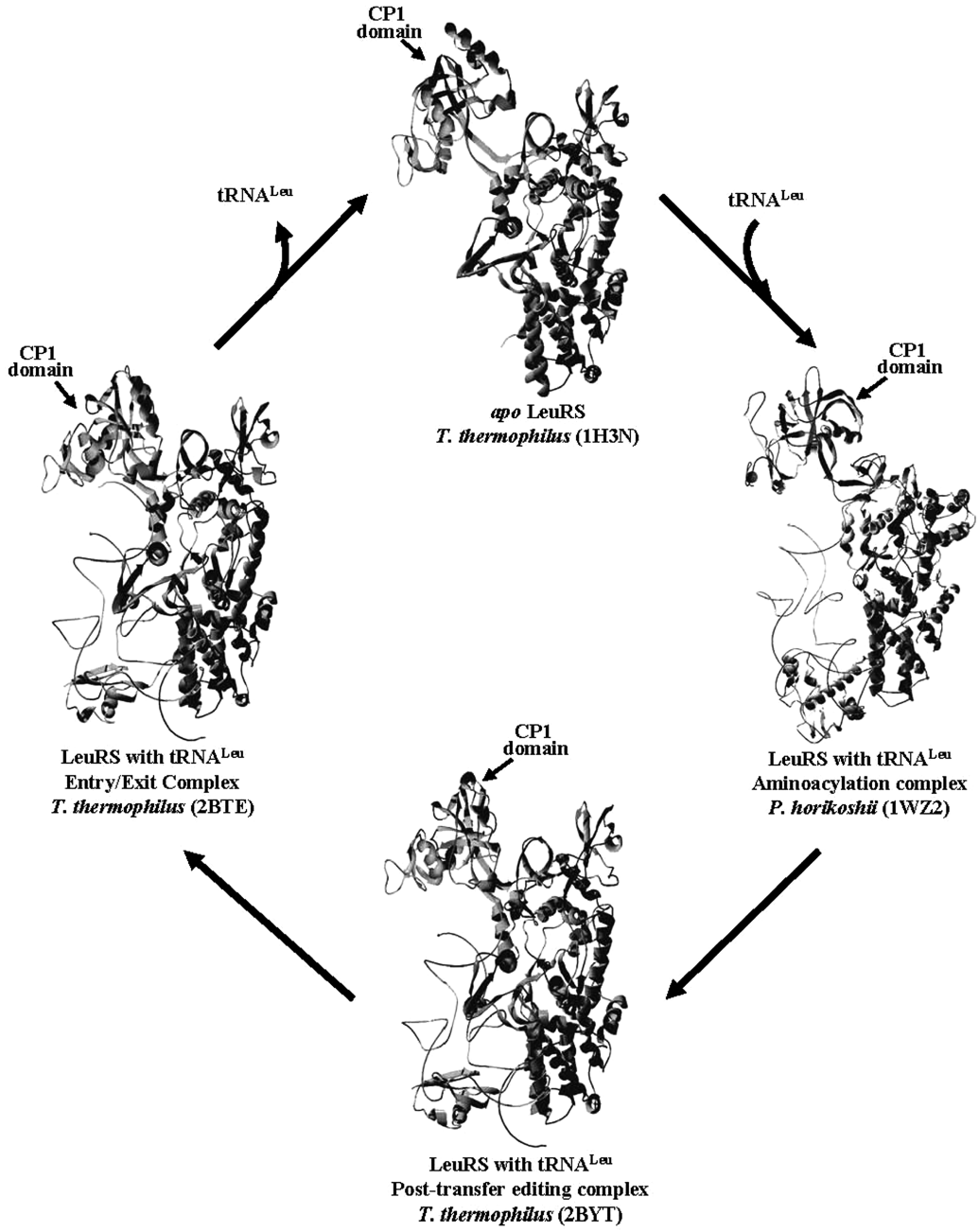

FIGURE 1: Tertiary structures of LeuRS. The enzyme cycle of LeuRS shows the apo X-ray crystal structure [top; Protein Data Bank (PDB) entry 1H3N], the aminoacylation cocrystal structure complex with tRNA (right; PDB entry 1WZ2), and the post-transfer editing cocrystal complex (bottom; PDB entry 2BYT). The exit complex, which has also been proposed to be an entry complex for tRNA binding (*30*), is shown at the left (PDB entry 2BTE). The LeuRS protein structure is displayed as a ribbon, while the bound tRNA is indicated as a distinct line. The CP1 domain is oriented at the top left of each structure as indicated by a marked arrow.

shows the 3′ end of the tRNA displaced from the editing active site is primed for release of tRNA from the enzyme.

We hypothesize that these rotations and orientations of the CP1 domain at various stages of the reaction pathway are dependent on the dynamic connecting β-strand linkers. The flexibility of the β-strands would also be required for translocation of the tRNA from the aminoacylation to the editing active site. To identify specific sites within the β-strand linkers that are important to the different steps of the enzyme's reaction cycle, we computationally investigated each of the linker peptides for specific hinge sites. We also created a series of two-amino acid deletions and tested each for alterations in aminoacylation, mischarging, and amino acid editing. We found that different sites within the C- and N-terminal β-strands preferentially impact aminoacylation over amino acid editing and vice versa.

EXPERIMENTAL PROCEDURES

Mutagenesis. The polymerase chain reaction (PCR) was carried out for deletion mutations and point mutations. Plasmid p15ec3-1 (*15*), which encodes the gene for wild-type *Escherichia coli* LeuRS, was used as a template. The 50 μL PCR mixture contained 200 ng of plasmid template, 125 ng of each forward and reverse primer (Integrated DNA Technologies, Coralville, IA), 0.2 mM dNTPs, and 0.05 unit of *Pfu* DNA polymerase (Stratagene, La Jolla, CA) in

commercially prepared buffer. The PCR mixture was restriction digested with 0.4 unit of *Dpn*I (Promega, Madison, WI) for 6 h at 37 °C and then used to transform *E. coli* DH5α (Stratagene). The mutated gene sequence was confirmed by DNA sequencing (UIUC Core Sequencing Facility, Urbana, IL).

Purification of E. coli LeuRS. Wild-type and mutant protein expression was induced with 1 mM IPTG (isopropyl β-D-thiogalactopyranoside) in *E. coli* strain BL21(DE3) *plysS* (Novagen, Madison, WI). The cells were harvested at 6000 rpm for 15 min in an Avanti J-E centrifuge (Beckman Coulter, Fullerton, CA). The cell pellet was resuspended in 5 mL of HA-I buffer [20 mM sodium phosphate (NaP_i), 10 mM tris(hydroxymethyl)aminomethane (Tris) (pH 8.0), 300 mM NaCl, and 5% glycerol]. Following sonication on ice for 2 min at 50% power using a Vibra Cell sonicator (Sonics, Newtown, CT), the lysate was centrifuged at 6000 rpm for 15 min at 4 °C. The supernatant was combined with 4 mL of resuspended HIS-Select HF Nickel Affinity gel (Sigma, St. Louis. MO), pre-equilibrated with HA-I buffer, and incubated for 1 h at 4 °C on a rocker. The resin was washed multiple times with a total of 100 mL of HA-I buffer that contained 5 mM imidazole. The protein was eluted with 10 mL of HA-I buffer containing 200 mM imidazole and concentrated in a Centricon-50 instrument (Amicon, Bedford, MA). The final concentration was determined using a Bio-Rad protein assay according to the commercial protocol (Bio-Rad Laboratories, Hercules, CA).

RNA Preparation. Plasmid ptDNALeu14 (*16, 17*), which harbors the gene for *E. coli* $tRNA^{Leu}_{UAA}$ ($tRNA^{Leu}$), was linearized by digesting 450 μg of the plasmid with *Bst*NI (New England Biolabs Inc., Beverly, MA) at 60 °C overnight and then used as a template for T7 RNA polymerase runoff transcription (*18*). The in vitro transcription reaction mixture contained 40 mM Tris (pH 8.0), 30 mM $MgCl_2$, 5 mM dithiothreitol (DTT), 0.01% Triton X-100, 50 μg/mL bovine serum albumin (BSA), each NTP at 4 mM, 80 mg/mL PEG8000, 0.02 unit/μL RNasin (Eppendorf, Hamburg, Germany), 2 mM spermidine, 0.4 mg/mL plasmid template, 0.01 mg/mL pyrophosphatase (Sigma), and 0.6 μM T7 RNA polymerase (*18, 19*). Reaction mixtures were incubated at 42 °C for 3 h, followed by addition of additional 0.6 μM T7 RNA polymerase and further incubation for 3 h. The reactions were quenched with 100% ethanol and the mixtures precipitated at −80 °C for at least 0.5 h.

The pelleted RNA was purified on a 10% denaturing polyacrylamide (19:1), 8 M urea gel by electrophoresis. The $tRNA^{Leu}$ band was detected by UV shadowing, excised, and crushed, and the RNA was extracted three times in a solution of 0.5 M NH_4OAc and 1 mM ethylenediaminetetraacetic acid (EDTA) (pH 8.0). After butanol extraction to concentrate the RNA, it was ethanol precipitated, and then the tRNA pellet was resuspended in 100 μL of nuclease free water (Ambion, Austin, TX). The concentration was calculated using an extinction coefficient of 840700 ($L\ mol^{-1}\ cm^{-1}$) for $tRNA^{Leu}$ (*20*).

Aminoacylation Assays. Reactions of 60 mM Tris (pH 7.5), 10 mM $MgCl_2$, 150 mM KCl, 1 mM DTT, 22 μM [^{3}H]leucine (167 μCi/mL; Amersham Pharmacia Biotech, Piscataway, NJ), 4 μM in vitro-transcribed *E. coli* $tRNA^{Leu}$, and catalytic amounts of enzyme were initiated with 4 mM ATP. Aliquots of 10 μL were quenched on Whatman filter pads, prewet with 5% trichloroacetic acid (TCA), at varying time intervals. The pads were washed three times for 10 min each with cold 5% TCA and then once with 70% ethanol. The washed pads were dried in anhydrous ether and then under a heat lamp. Radioactivity was quantified in a Beckman LS 6500 scintillation counter (Beckman Coulter). Apparent kinetic rate constants were measured by incorporating six different in vitro-transcribed $tRNA^{Leu}$ concentrations ranging from 0.1 to 10 μM. Using SigmaPlot (Systat Software, Inc., San Jose, CA), the kinetic parameters were calculated and error analysis was carried out.

Hydrolysis Assays. In vitro-transcribed *E. coli* $tRNA^{Leu}$ was misaminoacylated with [^{3}H]isoleucine (93 μCi/μL) (Amersham Pharmacia Biotech) by 1 μM *E. coli* LeuRS editing-deficient mutant as described above for 3 h at 37 °C. The reactions were quenched with 0.18% acetic acid (*21*). Protein was removed by extraction with a phenol/chloroform/isoamyl alcohol (125:24:1) mixture at pH 4.3. The RNA was ethanol precipitated and resuspended in 50 mM potassium phosphate buffer (pH 5.0).

Post-transfer editing activity was tested in reaction mixtures containing 60 mM Tris (pH 7.5), 10 mM $MgCl_2$, and approximately 4 μM [^{3}H]Ile-$tRNA^{Leu}$. Reactions were initiated with 100 nM enzyme. Aliquots of 5 μL were quenched on filter pads presoaked with 5% TCA, washed, and analyzed as described above.

Inorganic Pyrophosphate (PP_i) Exchange Assays. Reactions of 50 mM *N*-(2-hydroxyethyl)piperazine-*N*′-2-ethanesulfonic acid (HEPES) (pH 8.0), 10 mM $MgCl_2$, 1 mM DTT, 1 mM [^{32}P]PP_i (78 mCi/mL; Amersham Pharmacia Biotech), 1 mM leucine, and 100 nM enzyme were initiated with 1 mM ATP (*22*). Aliquots of 2 μL were quenched on cellulose polyethyleneimine (PEI) thin-layer chromatography (TLC) plates (Scientific Adsorbents Inc., Atlanta, GA) that were prerun in water. The reaction components were separated by developing the TLC plates in 750 mM KH_2PO_4 (pH 3.5) and 4 mM urea. Separated radiolabeled bands were detected using a phosphorimager and FUJIX BAS 1000 film (FUJIFILM Medical Systems U.S.A., Stanford, CT). Bands were quantitated with a Storm 840 molecular dynamics imager (GE Healthcare, Piscataway, NJ).

"Hinge" Prediction. We utilized the Morph Server (*23*) in the database of molecular motions (MolMovDB, www.molmovdb.org/) (*24*). This server characterizes macromolecular motions, by comparing two similar crystal structures as input. The tRNA coordinates in the crystal structures for *T. thermophilus* LeuRS in the post-transfer editing (PDB entry 2BYT) and exit (PDB entry 2BTE) complexes (*13*) were removed for comparative studies, and the remaining protein coordinates were uploaded into the single-chain Morph Server (*25*). A hinge predictor graph was developed using the output of FlexOracle (*26*), TLSMD (Translation/Liberation/Screw Motion Determination) (*27*), as well as a combined HingeMaster prediction.

Circular Dichroism. CD measurements were carried out using a Jasco J-720 spectropolarimeter. A sample containing 0.8 μM protein in 5 mM KP_i (pH 7.5) was measured in the far-ultraviolet region using a 0.1 cm path cell. Background signals from the cell and the buffer were subtracted from each spectrum.

RESULTS

Deletions Affect the Aminoacylation Activity of E. coli LeuRS. Multiple X-ray crystal structures and models suggest that the LeuRS CP1 domain adopts different conformations relative to the enzyme's canonical core as it moves between the aminoacylation and editing complexes with tRNA during its reaction cycle (Figure 1). We hypothesized that this rigid body movement of the CP1 domain would require coordinated movement of the flexible β-strand linkers. We compared the crystal structures of *T. thermophilus* LeuRS (PDB entries 2BTE and 2BYT) using the database of molecular motions (*24*) to identify potential residues that are sufficiently flexible to act as possible hinges. Three algorithms that predict highly flexible protein sites were employed to investigate LeuRS for hinge sites which might help drive the CP1 domain and canonical core into alternate conformations that were competent for aminoacylation and editing. Within the β-strands, a single hinge was predicted that corresponded to Ser227 at the N-terminus of the N-terminal β-strand (Figure 2A). This N-terminal β-strand serine site is highly conserved (Figure 2B). A second hinge between Glu393 and Ser394 was also predicted that was near the C-terminal β-strand but actually located within the CP1 domain. This latter hinge site is currently being analyzed in a separate investigation.

We hypothesized that the predicted hinge site at Ser227 within the N-terminal β-strand might facilitate conformational changes in the LeuRS that promoted aminoacylation, editing, or both. We introduced a series of two-amino acid deletions on the N-terminal β-strand of *E. coli* LeuRS beginning at the hinge site, Ser227 at its N-terminus (Figure 2B). These included a two-amino acid deletion, $\Delta S_{227}E_{228}$ at the predicted serine hinge site, as well as $\Delta G_{229}V_{230}$, $\Delta E_{231}I_{232}$, and $\Delta T_{233}F_{234}$, which spanned Ser227−Phe234 on the N-terminal β-strand. We also generated two-amino acid deletions on the C-terminal β-strand that encompassed $\Delta G_{407}V_{408}$, $\Delta G_{409}E_{410}$, $\Delta R_{411}K_{412}$, and $\Delta V_{413}N_{414}$ spanning Gly407−Asn414 (Figure 2B).

Each of the β-strand deletion mutants of LeuRS was stably expressed in *E. coli* and purified by affinity chromatography using an N-terminal six-histidine tag. The purified deletion mutants were then tested for aminoacylation activity with in vitro-transcribed $tRNA^{Leu}$. Only one mutant, the $\Delta S_{227}E_{228}$ LeuRS deletion that included the predicted hinge site on the N-terminal β-strand, failed to aminoacylate $tRNA^{Leu}$ (Table 1), even at high enzyme concentrations of 2 μM (data not shown). This mutant enzyme also did not activate amino acid in pyrophosphate exchange assays, suggesting that the conformation of the N-terminal β-strand influenced the aminoacylation active site directly (Figure 3A).

The $\Delta G_{229}V_{230}$ and $\Delta E_{231}I_{232}$ mutant LeuRSs retained significant aminoacylation activity compared to wild-type LeuRS, with k_{cat}/K_M values of 9.7 and 10.2 μM^{-1} s^{-1}, respectively (Table 1). The $\Delta T_{233}F_{234}$ LeuRS mutant activity was enhanced compared to that of wild-type LeuRS, largely due to an increase in k_{cat}. As would be expected and in contrast to the $\Delta S_{227}E_{228}$ mutation, each of these other deletion mutants maintained robust amino acid-dependent pyrophosphate exchange activity (Figure 3A).

Among the C-terminal β-strand deletion mutants, the k_{cat}/K_M for the $\Delta V_{413}N_{414}$ deletion mutant at the C-terminus of the C-terminal β-strand was the most significantly decreased compared to that of the wild-type enzyme. The 4-fold decrease was largely due to a modest decrease in the k_{cat} (Table 1). The $\Delta V_{413}N_{414}$ LeuRS deletion mutant displayed a lowered level of amino acid activation that correlated to its decrease in aminoacylation activity (Figure 3B). The $\Delta R_{411}K_{412}$ deletion mutant exhibited an elevated k_{cat}/K_M relative to that of the wild-type enzyme because of an increase in the k_{cat}. The $\Delta G_{407}V_{408}$ also had a slightly increased k_{cat}/K_M, while the $\Delta G_{409}E_{410}$ deletion mutant activity was similar to that of wild-type LeuRS.

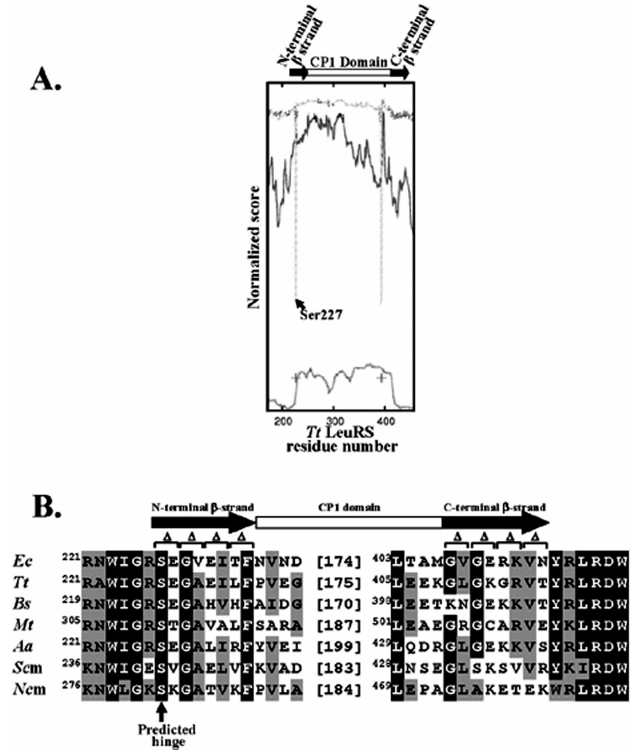

FIGURE 2: Hinge predictor graph and sequence alignment for LeuRS. (A) Hinge predictor graph for *T. thermophilus* LeuRS. The post-transfer editing (PDB entry 2BYT) and exit (PDB entry 2BTE) crystal structures for *T. thermophilus* LeuRS in the absence of $tRNA^{Leu}$ were compared using the Morph Server (*23*). The lines on the resulting graph are represented as follows: combined HingeMaster predictor by the upper trace where minima correspond to suggested hinge regions, FlexOracle prediction (*26*) in the middle with minima corresponding to hinges, and NSHP hinge predictor at the bottom. The TLSMD-predicted hinge residues (*27*) are indicated with a plus. The approximate locations of the CP1 and the connective linkers are depicted in the cartoon above the graph as an empty rectangle and shaded flanking arrows, respectively. (B) Sequence alignment of the CP1 domain and β-strand linkers. The N- and C-terminal β-strands are highlighted with shaded arrows. Two amino acid deletions for *E. coli* LeuRS are marked by the Δ signs. Black and gray shading denotes highly conserved and homologous residues, respectively. Abbreviations: *Ec*, *E. coli*; *Tt*, *T. thermophilus*; *Nc*m, *Neurospora crassa* (mitochondria); *Sc*m, *Saccharomyces cerevisiae* (mitochondria); *Bs*, *Bacillus subtilis*; *Hs*m, *Homo sapiens* (mitochondria); *Mt*, *Mycobacterium tuberculosis*; *Aa*, *Aquifex aeolicus* (α subunit). Sequence alignments were generated using the Baylor College of Medicine Search Launcher ClustalW 1.8 multiple-sequence alignment program (*34*).

Deletions Affect Post-Transfer Editing Activity of E. coli. Each of the two-amino acid deletion mutants was tested for amino acid editing activity of mischarged Ile-$tRNA^{Leu}$. Although it was inactive in aminoacylation, the $\Delta S_{227}E_{228}$ deletion mutant at the predicted hinge site on the N-terminal

Table 1: Apparent Kinetic Parameters for Aminoacylation[a]

	K_M (μM)	k_{cat} (s^{-1})	k_{cat}/K_M (μM^{-1} s^{-1})	relative k_{cat}/K_M
wild type	1.2 ± 0.2	14.3 ± 0.3	11.9	1
N-terminal β-strand				
$\Delta S_{227}E_{228}$	ND[b]	ND[b]	ND[b]	–
ΔS_{227}	ND[b]	ND[b]	ND[b]	–
ΔE_{228}	ND[b]	ND[b]	ND[b]	–
$\Delta G_{229}V_{230}$	0.94 ± 0.4	9.2 ± 2.7	9.7	0.8
$\Delta E_{231}I_{232}$	1 ± 0.1	10.2 ± 4	10.2	0.9
$\Delta T_{233}F_{234}$	2.3 ± 0.5	39.1 ± 3.3	17	1.4
C-terminal β-strand				
$\Delta G_{407}V_{408}$	0.9 ± 0.2	12.5 ± 1	13.8	1.2
$\Delta G_{409}E_{410}$	0.6 ± 0.1	6.9 ± 1.2	11.5	1
$\Delta R_{411}K_{412}$	2.1 ± 0.5	35.2 ± 3.5	16.7	1.4
$\Delta V_{413}N_{414}$	1.7 ± 0.6	4.5 ± 0.3	2.7	0.2
ΔV_{413}	0.7 ± 0.2	0.2 ± 0.05	0.3	0.02
ΔN_{414}	2.8 ± 0.5	0.6 ± 0.3	0.2	0.02

[a] Apparent rate constants were measured using leucine concentrations of 20 μM and in vitro-transcribed $tRNA^{Leu}$ ranging in concentration from 0.2 to 20 μM. [b] Not determined because of low activity.

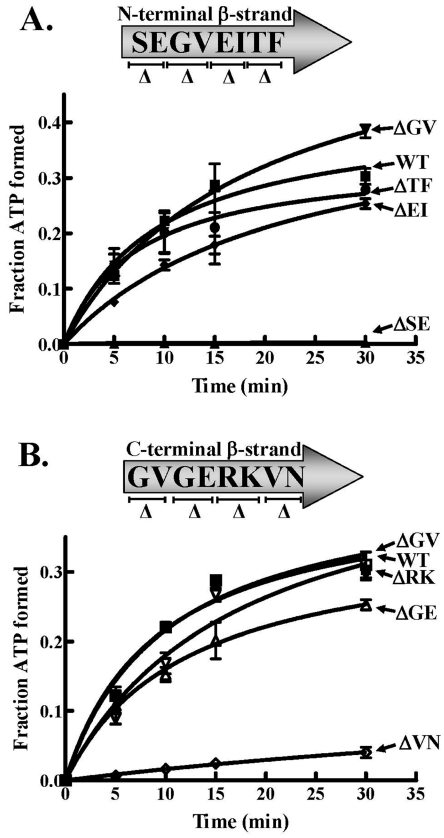

FIGURE 3: Leucine-dependent pyrophosphate exchange activities of wild-type LeuRS and β-strand two-amino acid deletion mutants. The reaction mixtures contained 100 nM wild-type or mutant LeuRS. (A) N-Terminal β-strand deletion mutant activities. (B) C-Terminal β-strand deletion mutant activities. Symbols are as follows: wild type (■), $\Delta S_{227}E_{228}$ (▲), $\Delta G_{229}V_{230}$ (▼), $\Delta E_{231}I_{232}$ (◆), $\Delta T_{233}F_{234}$ (●), $\Delta G_{407}V_{408}$ (□), $\Delta G_{409}E_{410}$ (△), $\Delta R_{411}K_{412}$ (▽), and $\Delta V_{413}N_{414}$ (◇). Error bars are the result of reactions repeated in triplicate and are indicated for each point.

β-strand exhibited some amino acid editing activity, albeit significantly reduced compared to the wild-type LeuRS activities (Figure 4A). We hypothesized that deletion of the Ser227 and Glu228 residues "kinks" the β-strands in such a way that allows tRNA binding in the editing complex, but not the aminoacylation complex. The other N-terminal β-strand deletion mutants exhibited slightly decreased hydrolysis rates that reached wild-type enzyme plateau levels. As previously determined for other LeuRS mutations that had only small decreases in editing activity (*28*), the N-terminal β-strand deletion mutants did not confer mischarging (data not shown). Although the $\Delta S_{227}E_{228}$ LeuRS had significantly decreased editing activity, its lack of mischarging activity was likely due to its failure to aminoacylate in general.

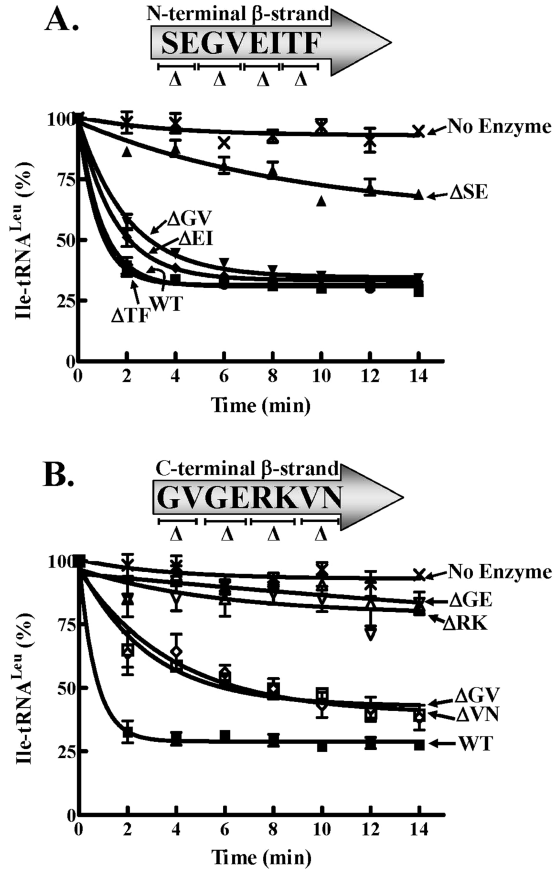

FIGURE 4: Amino acid editing activities of wild-type LeuRS and β-strand linker two-amino acid deletion mutants. The reactions of approximately 4 μM [^{3}H]Ile-$tRNA^{Leu}$ were initiated with 100 nM wild-type or mutant LeuRS. (A) N-Terminal β-strand deletion mutant activities. (B) C-Terminal β-strand deletion mutant activities. Symbols are as follows: wild type (■), $\Delta S_{227}E_{228}$ (▲), $\Delta G_{229}V_{230}$ (▼), $\Delta E_{231}I_{232}$ (◆), $\Delta T_{233}F_{234}$ (●), $\Delta G_{407}V_{408}$ (□), $\Delta G_{409}E_{410}$ (△), $\Delta R_{411}K_{412}$ (▽), $\Delta V_{413}N_{414}$ (◇), and no enzyme (×). Error bars are based on reactions that were repeated at least in triplicate.

In contrast to the N-terminal mutants, each of the C-terminal deletion mutants exhibited reduced amino acid editing activity relative to that of the wild-type enzyme. Although $\Delta R_{411}K_{412}$ on the C-terminal β-strand had wild-type-like aminoacylation activity, amino acid editing activity was significantly reduced (Figure 4B). The editing activity of $\Delta G_{409}E_{410}$ was also decreased like that of the $\Delta R_{411}K_{412}$ deletion mutant. While the $\Delta G_{407}V_{408}$ and $\Delta V_{413}N_{414}$ deletion mutants retained editing activity, neither attained plateau levels of hydrolysis of Ile-$tRNA^{Leu}$ that correlated to that of wild-type LeuRS.

Spatially Diverse Effects of β-Strand Linkers on Enzyme Activity. We compared the relative activities for aminoacylation and/or editing for each of the LeuRS deletion mutants and the wild type. We found spatial "hot spots" that influenced aminoacylation and editing on the N- and C-terminal β-strands. These sensitive areas on each β-strand

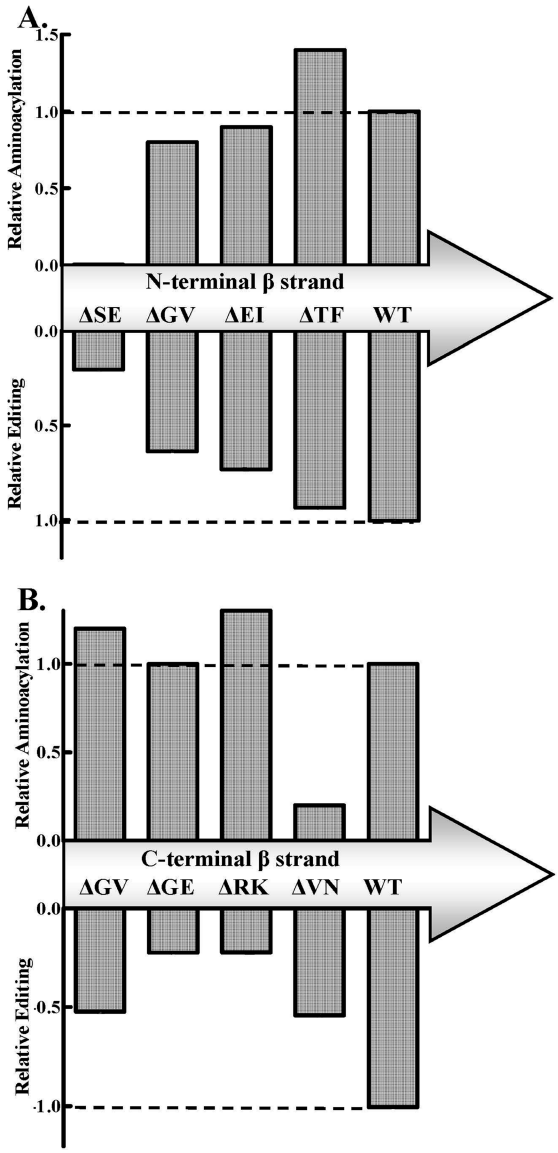

FIGURE 5: Relative aminoacylation and editing activities of deletion mutants on the β-strands of *E. coli* LeuRS: (A) N-terminal β-strand and (B) C-terminal β-strand. Aminoacylation activity (top) was normalized to wild-type aminoacylation activity based on the k_{cat}/K_M (Table 1), and values are shown in bar graph form. Estimates of the post-transfer editing activities (bottom) were normalized by comparing the hydrolyzed Ile-tRNA^{Leu} at the 2 min time point. The horizontal dashed line represents the activity of wild-type *E. coli* LeuRS.

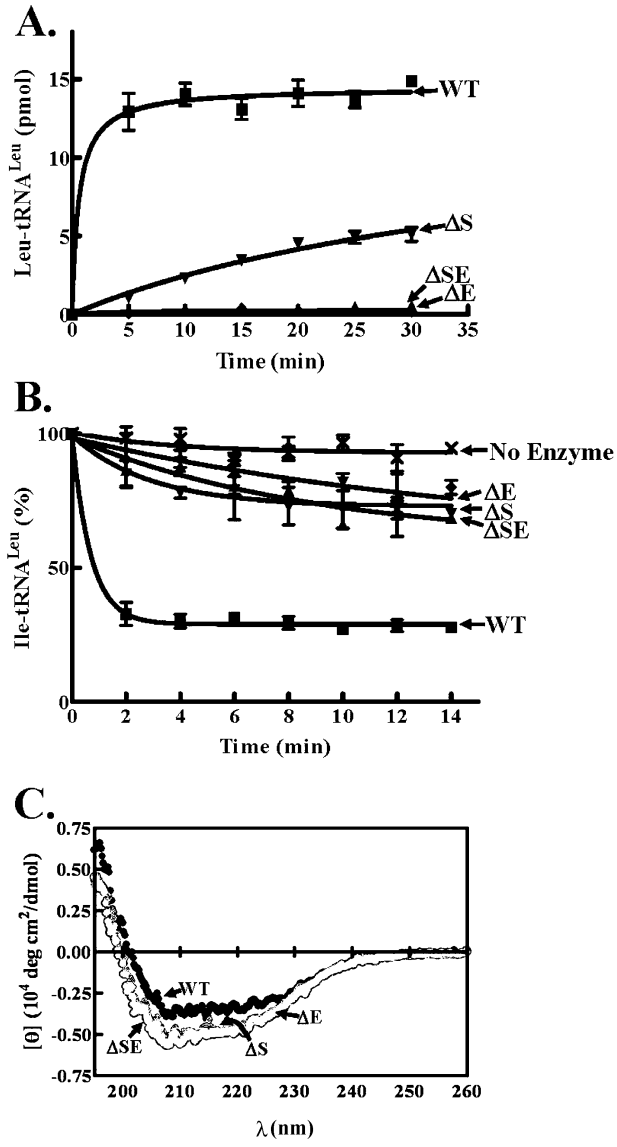

FIGURE 6: Enzymatic activities of wild-type LeuRS and N-terminal β-strand mutants. (A) Leucylation activities were measured using enzyme and tRNA^{Leu} concentrations of 50 nM and 4 μM, respectively. (B) Amino acid editing activities were determined using approximately 4 μM [^{3}H]Ile-tRNA^{Leu} and were initiated with 100 nM enzyme. Symbols are as follows: wild type (■), $\Delta S_{227}E_{228}$ (▲), ΔS_{227} (▼), ΔE_{228} (◆), and no enzyme (−). Error bars are the result of reactions repeated in triplicate and are indicated for each point. (C) CD spectra. The black symbols represent the wild-type LeuRS spectrum, while the gray symbols overlap for the spectra of the three deletion mutants.

linker were strikingly distinct. Deletions across the N-terminal β-strand determined that sites that were closer to the predicted hinge site near the canonical core of *E. coli* LeuRS more dramatically influenced both aminoacylation and editing activities (Figure 5A). We hypothesize that LeuRS requires more sequence specific flexibility at the β-strand end that is near the canonical core.

In contrast, deletions of the C-terminal β-strand showed diverse effects on aminoacylation and amino acid editing (Figure 5B). Each of the deletion mutants significantly impacted amino acid editing. Only the $\Delta V_{413}N_{414}$ LeuRS mutant at the end of the C-terminal β-strand near the canonical core influenced aminoacylation. The $\Delta G_{409}E_{410}$ and $\Delta R_{411}K_{412}$ LeuRS deletion mutants significantly reduced the editing activity of the enzyme but retained wild-type-like aminoacylation activity. It is possible that the C-terminal β-strand linker requires a flexible molecular hinge at the Val413-Asn414 site to form the aminoacylation complex.

Molecular Analysis of Aminoacylation Hot Spots on the β-Strand Linkers. We mutationally analyzed the two-amino acid deletion sites that exhibited the greatest impact on LeuRS activity. As found for the $\Delta S_{227}E_{228}$ deletion, single deletions of either amino acid reduced the level of both amino acid activation and aminoacylation. The ΔE_{228} LeuRS deletion mutant abolished aminoacylation, while the ΔS_{227} mutant retained detectable activity, albeit significantly reduced compared to that of wild-type LeuRS (Figure 6A). Despite repeated attempts, neither the kinetic parameters nor the k_{cat}/K_M could be reproducibly measured.

The extent of hydrolysis of Ile-tRNA^{Leu} by each of the single-deletion mutants was also substantially decreased

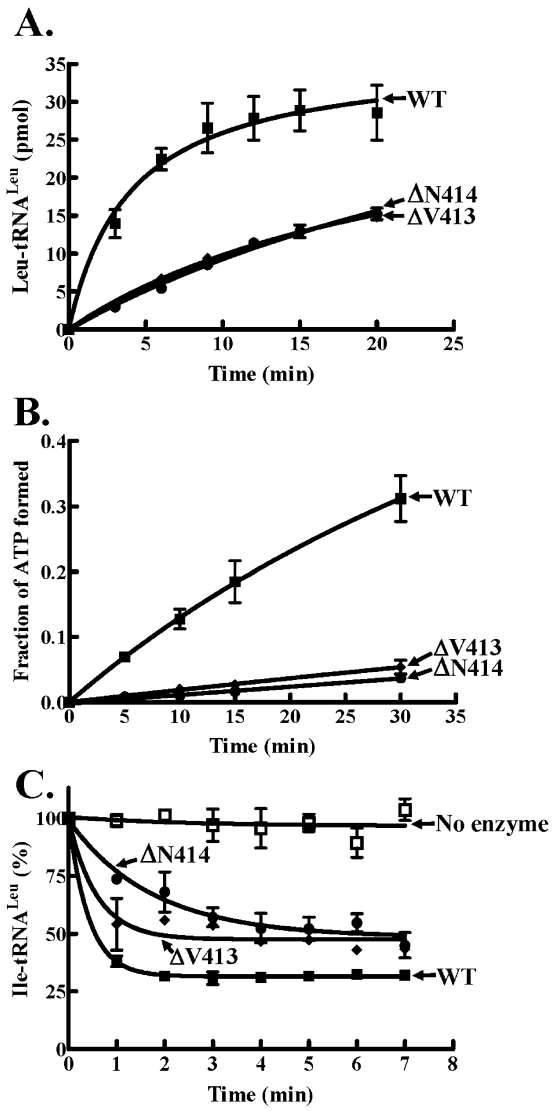

FIGURE 7: Enzymatic activities of wild-type LeuRS and C-terminal single-deletion β-strand mutants. (A) Leucylation activities were measured using enzyme concentrations of 50 nM. (B) Leucine-dependent pyrophosphate exchange activities were determined using 100 nM enzyme. (C) Amino acid editing activities were determined using approximately 4 μM [^{3}H]Ile-tRNA^{Leu} and were initiated with 100 nM enzyme. Symbols are as follows: wild type (■), ΔV_{413} (◆), ΔN_{414} (●), and no enzyme (□). Error bars are the result of reactions repeated in triplicate and are indicated for each point.

similar to that of the $\Delta S_{227}E_{228}$ LeuRS deletion mutant (Figure 6B). We tested whether mutations at this critical hinge site cause structural deformities. However, the CD spectrum of each of the deletion mutants at Ser227 and Glu228 showed that their secondary structures compared well to the wild-type enzyme (Figure 6C).

We also constructed single-deletion mutations at the Val413 and Asn414 sites within the C-terminal β-strand. These mutants retain a robust editing activity (Figure 7), which maintains fidelity of the LeuRS even though it is decreased compared to that of the wild-type enzyme. This is consistent with previously reported mutations in the editing active site that had decreased post-transfer editing activity (*28*).

The individual deletions at Val413 and Asn414 significantly decreased aminoacylation activity 50-fold (Table 1). This was primarily due to a k_{cat} effect. Surprisingly, the k_{cat} and k_{cat}/K_M for the double $\Delta V_{413}N_{414}$ mutant were at least 10-fold higher compared to those of the single mutations. It has been proposed that turnover of the class I enzymes is limited by product release (*29*). It is possible that the more extensive deletion of two amino acids relative to the single deletions destabilized tRNA translocation or the so-called exit complex (*13*) to facilitate premature product release. However, the mechanistic bases of the more dramatic effects on the single-deletion versus the double-deletion mutants of Val413 and Asn414 remain unclear.

Pyrophosphate exchange activity was also greatly decreased for each of the ΔV_{413} and ΔN_{414} single mutants. This effect was similar to that of the $\Delta V_{413}N_{414}$ LeuRS double mutant as well as deletions at Ser227 and Glu228 that are described above. Thus, mutations in the β-strand linkers not only affect LeuRS conformations that interact with the tRNA but also distally influence amino acid binding in the synthetic aminoacylation site.

DISCUSSION

Translocation of the 3′-charged end between the aminoacylation active site in the canonical core and the CP1 domain-based hydrolytic site occurs via a mechanism that remains virtually undefined. The accumulation of numerous LeuRS crystal structures (*2*) shows clearly that the enzyme undergoes significant conformational changes to accommodate the aminoacylation and the editing complexes. This is also accompanied by changes in the tRNA, particularly at the 3′ end that is charged, and its interactions with the AARS.

It is likely that LeuRS translocation is pseudoreversible such that the tRNA's 3′ end can move from the editing active site to the aminoacylation active site and naturally occurs as an obligatory part of the enzyme's reaction cycle. Recently, a boron containing inhibitor that binds in the LeuRS editing active site, AN2690, was shown to covalently trap the 3′ end of the tRNA in the editing complex (*30*). Surprisingly, AN2690 cross-linking occurs quite effectively with uncharged tRNA in the absence of leucine and/or ATP. This suggests that the uncharged 3′ end of the tRNA sweeps through the editing site enroute to binding to the aminoacylation active site. This result also raises the possibility that the so-called exit complex structure (*13*) of LeuRS bound to tRNA^{Leu} also serves as an entrance complex for tRNA binding (*30*). In the exit complex, the charged 3′ end of the tRNA resides near the editing active site (*13*). If the entrance complex resembles the exit complex, then we might expect the tRNA's 3′ end to transiently occupy the editing active site as it undergoes the transition to the aminoacylation active site. Once charged, the tRNA would be translocated back to the editing complex for proofreading and, if necessary, editing. Subsequent to screening by the hydrolytic editing active site, the correctly charged tRNA would undergo the transition to the exit complex, prior to release.

These dynamic transitions would be expected to require coordinated movement by the enzyme and tRNA. We hypothesized that LeuRS, ValRS, and IleRS require the flexible β-strand linkers to act as hinges to direct these conformational changes. Computational analysis indicated that the N-terminus of the N-terminal β-strand linker to the mobile CP1 domain may act as such a hinge. Deletion mutations at positions Ser227 and Glu228 drastically affected aminoacylation but retained small amounts of amino acid editing activity. In addition,

neighboring two-amino acid deletions appear to have an interrelated effect on aminoacylation and post-transfer editing efficiency that declined as the disruptions sequentially moved away from the main body of the enzyme on the N-terminal β-strand and toward the CP1 domain (Figure 5).

In the cocrystal structure of *T. thermophilus* LeuRS bound to $tRNA^{Leu}$ in an exit complex, the ribose of Cyt74 interacts with Ser227 (*13*). When the transition to an editing complex is undergone, the 3′ acceptor stem of tRNA is reoriented along with a 5° rotation of the CP1 domain (*13*). The deletion of Ser227 would disrupt this interaction near the editing active site. If the tRNA entry complex resembles the tRNA exit complex, then we would also expect tRNA binding to be disrupted, precluding formation of an active aminoacylation complex.

The N-terminal β-strand is flanked by the mobile zinc-containing ZN-1 domain, which appears to sterically impede a conformational transition of the tRNA to the aminoacylation complex (*13*). This domain adopts open and closed conformations, where the closed position blocks entry of the 3′ end of tRNA into the catalytic site for aminoacylation but does not impede post-transfer editing (*13*). Deletions at Ser227 and Glu228 could result in a structural conformation that hampers movement of the adjacent ZN-1 domain. Thus, an active aminoacylation complex would be blocked; however, an editing complex could be formed that stimulates at least some deacylation activity as found for ΔS_{227} and $\Delta S_{227}E_{228}$ mutant enzymes.

The C-terminal β-strand is flanked by the CP1 editing domain and the conserved "RDW" region on the canonical core of the enzyme (*31*). This RDW peptide interacts with tRNA in various conformations and may position tRNA for different enzyme activities (*31*). A model based on the *T. thermophilus* and *P. horikoshii* enzyme−tRNA complexes suggests that the RDW peptide positions the 3′ end of tRNA for transition to an aminoacylation complex (*13*). Disruption of this interaction could account for the aminoacylation deficient $\Delta V_{413}N_{414}$ LeuRS deletion mutant that retains amino acid editing and is located the closest to the RDW peptide. In addition, in the exit−entry complex of *T. thermophilus* LeuRS, Arg418 (Arg416 in *E. coli*) of this peptide interacts with Ade73 of the tRNA (*13*). The robust aminoacylation activity of deletion mutants spanning Gly407−Lys412 could come at a cost to the enzyme's editing activity by "trapping" the CP1 editing domain in an aminoacylation conformation.

Hinge sites for facilitating the movement of editing substrates between the aminoacylation and editing active site have also been characterized for IleRS (*32*). Substitutions at proposed hinge sites within the canonical core of the homologous IleRS (Lys183 and Trp421) affect translocation and, thereby, the overall editing of the enzyme (*32*). It was proposed that these mutations impeded the CP1 domain movement that would be required for editing to occur. This hinge lysine is also conserved in LeuRS and plays a clear role in the fidelity mechanisms of *E. coli* LeuRS (*33*). It was hypothesized that this surface lysine on the canonical core of LeuRS interacts with negatively charged amino acids on the CP1 domain surface to stabilize one or more of the enzyme's conformations during the reaction cycle.

Communication between the CP1 domain and the core of the enzyme, at various phases of enzyme activity, is dependent on the β-strands that link them. Structural evidence suggests that the concerted movements of the ZN-1 and CP1 domains relative to the canonical core are likely orchestrated by the 3′ end of tRNA (*13*). The different orientations adopted by the enzyme would require that movement of the ZN-1 and CP1 domains coincide with changes at flexible hinge sites within the β-strands.

ACKNOWLEDGMENT

We are grateful to Dr. Stephen Cusack for valuable discussions and technical advice.

REFERENCES

1. Ibba, M., Francklyn, C., and Cusack, S., Eds. (2005) *Aminoacyl-tRNA Synthetases* Landes Bioscience/Eurekah.com, Georgetown, TX.
2. Mascarenhas, A. P., An, S., Rosen, A. E., Martinis, S. A., and Musier-Forsyth, K. (2008) Fidelity mechanisms of the aminoacyl-tRNA synthetases, in *Protein Engineering* (RajBhandary, U. L., and Kohrer, C., Eds.) Springer-Verlag, Berlin (in press).
3. Hendrickson, T. L., and Schimmel, P. (2003) Transfer RNA-dependent amino acid discrimination by aminoacyl-tRNA synthetases, in *Translation Mechanisms* (Lapointe, J., and Brakier-Gingras, L., Eds.) pp 35–64, Kluwer Academic/Plenum Publishers, Dordrecht, The Netherlands.
4. Zhang, C. M., Perona, J. J., and Hou, Y. M. (2003) Amino acid discrimination by a highly differentiated metal center of an aminoacyl-tRNA synthetase. *Biochemistry 42*, 10931–10937.
5. Pauling, L. (1958) The probability of errors in protein synthesis, in *Festschrift Arthur Stoll Siebzigsten Geburtstag*, pp 597602.
6. Fersht, A. R. (1977) Editing mechanisms in protein synthesis. Rejection of valine by the isoleucyl-tRNA synthetase. *Biochemistry 16*, 1025–1030.
7. Hati, S., Ziervogel, B., Sternjohn, J., Wong, F. C., Nagan, M. C., Rosen, A. E., Siliciano, P. G., Chihade, J. W., and Musier-Forsyth, K. (2006) Pre-transfer editing by class II prolyl-tRNA synthetase: Role of aminoacylation active site in "selective release" of noncognate amino acids. *J. Biol. Chem. 281*, 27862–27872.
8. O'Donoghue, P., and Luthey-Schulten, Z. (2003) On the evolution of structure in aminoacyl-tRNA synthetases. *Microbiol. Mol. Biol. Rev. 67*, 550–573.
9. Cusack, S., Yaremchuk, A., and Tukalo, M. (2000) The 2 Å crystal structure of leucyl-tRNA synthetase and its complex with a leucyl-adenylate analogue. *EMBO J. 19*, 2351–2361.
10. Nureki, O., Vassylyev, D. G., Tateno, M., Shimada, A., Nakama, T., Fukai, S., Konno, M., Hendrickson, T. L., Schimmel, P., and Yokoyama, S. (1998) Enzyme structure with two catalytic sites for double-sieve selection of substrate. *Science 280*, 578–582.
11. Fukai, S., Nureki, O., Sekine, S., Shimada, A., Tao, J., Vassylyev, D. G., and Yokoyama, S. (2000) Structural basis for double-sieve discrimination of L-valine from L-isoleucine and L-threonine by the complex of tRNA(Val) and valyl-tRNA synthetase. *Cell 103*, 793–803.
12. Starzyk, R. M., Burbaum, J. J., and Schimmel, P. (1989) Insertion of new sequences into the catalytic domain of an enzyme. *Biochemistry 28*, 8479–8484.
13. Tukalo, M., Yaremchuk, A., Fukunaga, R., Yokoyama, S., and Cusack, S. (2005) The crystal structure of leucyl-tRNA synthetase complexed with $tRNA^{Leu}$ in the post-transfer-editing conformation. *Nat. Struct. Mol. Biol. 12*, 923–930.
14. Fukunaga, R., and Yokoyama, S. (2005) Aminoacylation complex structures of leucyl-tRNA synthetase and $tRNA^{Leu}$ reveal two modes of discriminator base recognition. *Nat. Struct. Mol. Biol. 12*, 915–922.
15. Martinis, S. A., and Fox, G. E. (1997) Non-standard amino acid recognition by *Escherichia coli* leucyl-tRNA synthetase. *Nucleic Acids Symp. Ser. 36*, 125–128.
16. Tocchini-Valentini, G., Saks, M. E., and Abelson, J. (2000) tRNA leucine identity and recognition sets. *J. Mol. Biol. 298*, 779–793.
17. Normanly, J., Ogden, R. C., Horvath, S. J., and Abelson, J. (1986) Changing the identity of a transfer RNA. *Nature 321*, 213–219.

18. Sampson, J. R., and Uhlenbeck, O. C. (1988) Biochemical and physical characterization of an unmodified yeast phenylalanine transfer RNA transcribed *in vitro*. *Proc. Natl. Acad. Sci. U.S.A. 85*, 1033–1037.
19. Grodberg, J., and Dunn, J. J. (1988) ompT encodes the *Escherichia coli* outer membrane protease that cleaves T7 RNA polymerase during purification. *J. Bacteriol. 170*, 1245–1253.
20. Zhai, Y., and Martinis, S. A. (2005) Two conserved threonines collaborate in the *Escherichia coli* leucyl-tRNA synthetase amino acid editing mechanism. *Biochemistry 44*, 15437–15443.
21. Schreier, A. A., and Schimmel, P. R. (1972) Transfer ribonucleic acid synthetase catalyzed deacylation of aminoacyl transfer ribonucleic acid in the absence of adenosine monophosphate and pyrophosphate. *Biochemistry 11*, 1582–1589.
22. Lincecum, T. L., and Martinis, S. A. (2000) The tRNA Synthetase Proofreading and Editing Active Sites: A Novel Antibiotic Target. *SAAS Bull. Biochem. Biotechnol. 13*, 25–33.
23. Flores, S., Echols, N., Milburn, D., Hespenheide, B., Keating, K., Lu, J., Wells, S., Yu, E. Z., Thorpe, M., and Gerstein, M. (2006) The Database of Macromolecular Motions: New features added at the decade mark. *Nucleic Acids Res. 34*, D296–D301.
24. Gerstein, M., and Krebs, W. (1998) A database of macromolecular motions. *Nucleic Acids Res. 26*, 4280–4290.
25. Krebs, W. G., and Gerstein, M. (2000) The morph server: A standardized system for analyzing and visualizing macromolecular motions in a database framework. *Nucleic Acids Res. 28*, 1665–1675.
26. Flores, S. C., and Gerstein, M. B. (2007) FlexOracle: Predicting flexible hinges by identification of stable domains. *BMC Bioinf. 8*, 215.
27. Painter, J., and Merritt, E. A. (2005) A molecular viewer for the analysis of TLS rigid-body motion in macromolecules. *Acta Crystallogr. D61*, 465–471.
28. Mursinna, R. S., and Martinis, S. A. (2002) Rational design to block amino acid editing of a tRNA synthetase. *J. Am. Chem. Soc. 124*, 7286–7287.
29. Zhang, C. M., Perona, J. J., Ruy, K., Francklyn, C. S., and Hou, Y. M. (2006) Distinct kinetic mechanisms of the two classes of aminoacyl-tRNA synthetases. *J. Mol. Biol. 361*, 300–311.
30. Rock, F. L., Mao, W., Yaremchuk, A., Tukalo, M., Crepin, T., Zhou, H., Zhang, Y. K., Hernandez, V., Akama, T., Baker, S. J., Plattner, J. J., Shapiro, L., Martinis, S. A., Benkovic, S. J., Cusack, S., and Alley, M. R. K. (2007) An antifungal agent inhibits an aminoacyl-tRNA synthetase by trapping tRNA in the editing site. *Science 316*, 1759–1761.
31. Nawaz, M. H., Pang, Y. L., and Martinis, S. A. (2007) Molecular and functional dissection of a putative RNA-binding region in yeast mitochondrial leucyl-tRNA synthetase. *J. Mol. Biol. 367*, 384–394.
32. Bishop, A. C., Beebe, K., and Schimmel, P. R. (2003) Interstice mutations that block site-to-site translocation of a misactivated amino acid bound to a class I tRNA synthetase. *Proc. Natl. Acad. Sci. U.S.A. 100*, 490–494.
33. Williams, A. M., and Martinis, S. A. (2006) Mutational unmasking of a tRNA-dependent pathway for preventing genetic code ambiguity. *Proc. Natl. Acad. Sci. U.S.A. 103*, 3586–3591.
34. Smith, R. F., Wiese, B. A., Wojzynski, M. K., Davison, D. B., and Worley, K. C. (1996) BCM Search Launcher: An integrated interface to molecular biology data base search and analysis services available on the World Wide Web. *Genome Res. 6*, 454–462.

BI702494Q